Interfacial Self-Organization of Bolaamphiphiles Bearing Mesogenic Groups: Relationships between the Molecular Structures and Their Self-Organized Morphologies

ARTICLE *in* LANGMUIR · MAY 2008

Impact Factor: 4.46 · DOI: 10.1021/la7030158 · Source: PubMed

6 AUTHORS, INCLUDING:

Bo Song
Soochow University (PRC)
52 PUBLICATIONS **726** CITATIONS
SEE PROFILE

Shouchun Yin
Hangzhou Normal University
37 PUBLICATIONS **734** CITATIONS
SEE PROFILE

Zhiqiang Wang
Wuhan University
179 PUBLICATIONS **8,334** CITATIONS
SEE PROFILE

Interfacial Self-Organization of Bolaamphiphiles Bearing Mesogenic Groups: Relationships between the Molecular Structures and Their Self-Organized Morphologies

Bo Song, Guanqing Liu, Rui Xu, Shouchun Yin, Zhiqiang Wang,* and Xi Zhang*

Key Lab of Organic Optoelectronics and Molecular Engineering, Department of Chemistry, Tsinghua University, Beijing 100084, People's Republic of China

Received October 1, 2007. In Final Form: December 15, 2007

This article discusses the relationship between the molecular structure of bolaamphiphiles bearing mesogenic groups and their interfacial self-organized morphology. On the basis of the molecular structures of bolaamphiphiles, we designed and synthesized a series of molecules with different hydrophobic alkyl chain lengths, hydrophilic headgroups, mesogenic groups, and connectors between the alkyl chains and the mesogenic group. Through investigating their interfacial self-organization behavior, some experiential rules are summarized: (1) An appropriate alkyl chain length is necessary to form stable surface micelles; (2) different categories of headgroups have a great effect on the interfacial self-organized morphology; (3) different types of mesogenic groups have little effect on the structure of the interfacial assembly when it is changed from biphenyl to azobenzene or stilbene; (4) the orientation of the ester linker between the mesogenic group and alkyl chain can greatly influence the interfacial self-organization behavior. It is anticipated that this line of research may be helpful for the molecular engineering of bolaamphiphiles to form tailor-made morphologies.

Introduction

The interfacial self-organization of amphiphiles can produce various two-dimensional supramolecular nanostructures,[1−6] which have the potential to be used as lateral nanomaterials or templates of biomimetic or biomineralization processes.[7−10] Research in this field started as early as 1955, when Gaudin and Fuerstenau proposed the formation of hemimicelles at the solid/liquid interface based on the adsorption isotherms of single-headed ionic surfactants.[11] To elucidate the unusual adsorption phenomena of surfactants, the "two-step" model and the "four-region" model have been proposed to interpret the isotherms theoretically and qualitatively.[12−15] Both models assume that formation of the monolayer and bilayer depends on the adsorption amount at different concentrations. One breakthrough in this area is the direct observation of the tetradecyl trimethylammonium bromide adsorption structure at solid/liquid interfaces by Manne et al. using in-situ AFM with noncontact mode.[16,17] From then on, the interfacial self-organization of the amphiphilic molecules has been widely studied as well as the factors that can influence the formation of organized structures.[18−31]

About 20 years ago, a new type of amphiphile with two hydrophilic heads covalently connected by one hydrophobic chain was synthesized[32,33] and named bolaamphiphile by Fuhrhop et al.[34,35] Since then, much more scientific attention has focused on studying the self-organization behavior of bolaamphiphiles.[36−49]

* To whom correspondence may be addressed. Fax: +86-010-62771149. E-mail: xi@mail.tsinghua.edu.cn.

(1) Ringsdorf, H.; Schlarb, B.; Venzmer, J. *Angew. Chem., Int. Ed.* **1988**, *27*, 113−158.
(2) Ahlers, M.; Mueller, W.; Reichert, A.; Ringsdorf, H.; Venzmer, J. *Angew. Chem., Int. Ed.* **1990**, *29*, 1269−1285.
(3) Kunitake, T. *Angew. Chem., Int. Ed.* **1992**, *31*, 709−726.
(4) Oshovsky, G. V.; Reinhoudt, D. N.; Verboom, W. *Angew. Chem., Int. Ed.* **2007**, *46*, 2366−2393.
(5) Karaborni, S.; Esselink, K.; Hilbers, P. A. J.; Smit, B.; Karthauser, J.; Vanos, N. M.; Zana, R. *Science* **1994**, *266*, 254−256.
(6) Mao, G. Z.; Tsao, Y. H.; Tirrell, M.; Davis, H. T.; Hessel, V.; Ringsdorf, H. *Langmuir* **1993**, *9*, 3461−3470.
(7) Aksay, I. A.; Trau, M.; Manne, S.; Honma, I.; Yao, N.; Zhou, L.; Fenter, P.; Eisenberger, P. M.; Gruner, S. M. *Science* **1996**, *273*, 892−898.
(8) Luk, Y. Y.; Abbott, N. L. *Curr. Opin. Colloid Interface Sci.* **2002**, *7*, 267−275.
(9) Berti, D. *Curr. Opin. Colloid Interface Sci.* **2006**, *11*, 74−78.
(10) Shimizu, T.; Masuda, M.; Minamikawa, H. *Chem. Rev.* **2005**, *105*, 1401−1443.
(11) Gaudin, A. W.; Fuerstenau, D. W. *Trans. AIME* **1955**, *202*, 958−962.
(12) Fan, A. X.; Somasundaran, P.; Turro, N. J. *Langmuir* **1997**, *13*, 506−510.
(13) Zhu, B. Y.; Gu, T. R. *J. Chem. Soc., Farady Trans. 1* **1989**, *85*, 3813−3817.
(14) Zhu, B. Y.; Gu, T. R. *J. Chem. Soc., Farady Trans. 1* **1989**, *85*, 3819−3824.
(15) Atkin, R.; Craig, V. S. J.; Wanless, E. J.; Biggs, S. *Adv. Colloid Interface Sci.* **2003**, *103*, 219−304.
(16) Manne, S.; Cleveland, J. P.; Gaub, H. E.; Stucky, G. D.; Hansma, P. K. *Langmuir* **1994**, *10*, 4409−4413.
(17) Manne, S.; Gaub, H. E. *Science* **1995**, *270*, 1480−1482.
(18) Chavez, P.; Ducker, W.; Israelachvili, J.; Maxwell, K. *Langmuir* **1996**, *12*, 4111−4115.
(19) Lamont, R. E.; Ducker, W. A. *J. Am. Chem. Soc.* **1998**, *120*, 7602−7607.
(20) Wanless, E. J.; Ducker, W. A. *J. Phys. Chem.* **1996**, *100*, 3207−3214.
(21) Wanless, E. J.; Davey, T. W.; Ducker, W. A. *Langmuir* **1997**, *13*, 4223−4228.
(22) Liu, J. F.; Min, G.; Ducker, W. A. *Langmuir* **2001**, *17*, 4895−4903.
(23) Tulpar, A.; Ducker, W. A. *J. Phys. Chem. B* **2004**, *108*, 1667−1676.
(24) Khan, A.; Ducker, W. A.; Mao, M. *J. Phys. Chem. B* **2006**, *110*, 23365−23372.
(25) Manne, S.; Schaffer, T. E.; Huo, Q.; Hansma, P. K.; Morse, D. E.; Stucky, G. D.; Aksay, I. A. *Langmuir* **1997**, *13*, 6382−6387.
(26) Jaschke, M.; Butt, H. J.; Gaub, H. E.; Manne, S. *Langmuir* **1997**, *13*, 1381−1384.
(27) Patrick, H. N.; Warr, G. G.; Manne, S.; Aksay, I. A. *Langmuir* **1997**, *13*, 4349−4356.
(28) Patrick, H. N.; Warr, G. G.; Manne, S.; Aksay, I. A. *Langmuir* **1999**, *15*, 1685−1692.
(29) Wolgemuth, J. L.; Workman, R. K.; Manne, S. *Langmuir* **2000**, *16*, 3077−3081.
(30) Davey, T. W.; Ducker, W. A.; Hayman, A. R. *Langmuir* **2000**, *16*, 2430−2435.
(31) Zana, R. *J. Colloid Interface Sci.* **2002**, *252*, 259−261.
(32) Kunitake, T.; Okahata, Y. *J. Am. Chem. Soc.* **1977**, *99*, 3860−3861.
(33) Okahata, Y.; Kunitake, T. *J. Am. Chem. Soc.* **1979**, *101*, 5231−5234.
(34) Fuhrhop, J. H.; David, H. H.; Mathieu, J.; Liman, U.; Winter, H. J.; Boekema, E. *J. Am. Chem. Soc.* **1986**, *108*, 1785−1791.
(35) Fuhrhop, J. H.; Liman, U. *J. Am. Chem. Soc.* **1984**, *106*, 4643−4644.
(36) Fuhrhop, J. H.; Wang, T. Y. *Chem. Rev.* **2004**, *104*, 2901−2937.
(37) Fuhrhop, J. H.; Helfrich, W. *Chem. Rev.* **1993**, *93*, 1565−1582.
(38) Fuhrhop, J. H.; Spiroski, D.; Boettcher, C. *J. Am. Chem. Soc.* **1993**, *115*, 1600−1601.
(39) Fuhrhop, J. H.; Svenson, S.; Boettcher, C.; Roessler, E.; Vieth, H. M. *J. Am. Chem. Soc.* **1990**, *112*, 4307−4312.
(40) Mock, R. S.; Grimsrud, E. P. *J. Am. Chem. Soc.* **1989**, *111*, 2861−2870.

10.1021/la7030158 CCC: $40.75
Published on Web 03/08/2008 PAGE EST: 5.7

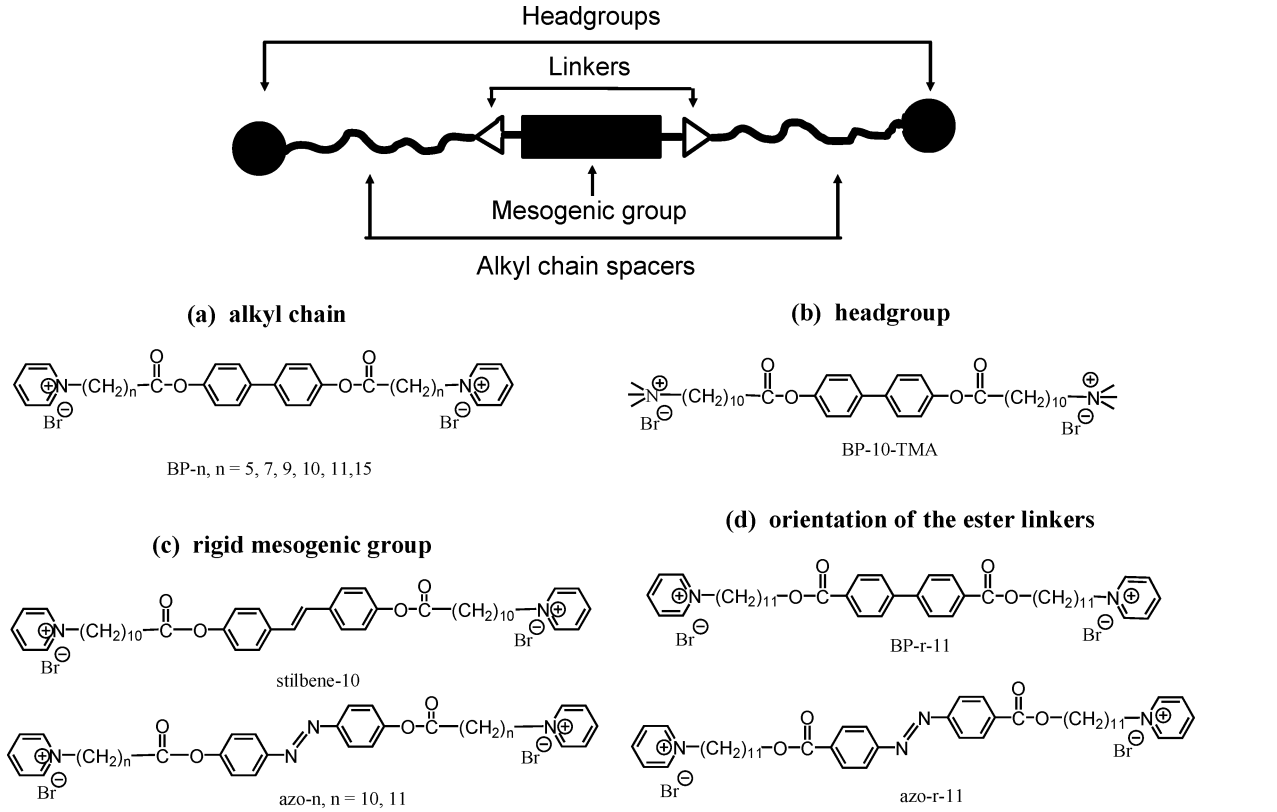

Figure 1. Schematic illustration of the bolaamphiphile bearing a mesogenic group and diversified bolaamphiphilic molecules involved: (a) similar bolaamphihiles with different alkyl chain length; (b) similar bolaamphihiles with different headgroups; (c) similar bolaamphihiles with different mesogenic groups; (d) similar bolaamphihiles with the orientation of the carbonyl group directly attached to the mesogenic groups, which is different from the bolaamphiphile shown in c.

In our previous work, we introduced mesogenic groups in between the alkyl chains of the bolaamphiphiles, studied their interfacial self-organization behavior, and demonstrated that, unlike the normal amphiphiles, their interfacial micellar structures are stable enough during the drying process.[50−56] Besides introduction of mesogenic groups to bolaamphihiles, we also tried to introduce strong $\pi-\pi$ stacking moieties into bolaamphiphiles and obtained stable supramolecular nanostrcutres.[57,58] These methods might be developed as a facile way to fabricate nanoscale-patterned surfaces. Since self-organization happens spontaneously at the interface as a consequence of hydrophobic[59] and other supramolecular interactions, how can one control the formation of self-organized structures? There might be some external conditions to adjust, such as the solvent and solution conditions (pH and temperature), the electrolytes competing with the amphiphiles for the surface, and the nature of the adsorbing surface. Besides the above parameters, the molecular feature is the most dominating factor in determining the resulting interfacial self-organized morphology and stability. Thus, revealing the relationship between the molecular structure and their self-organized morphologies could help us design the target amphiphilic molecules according to our needs.

As depicted in Figure 1, the structure of bolamphiphiles is comprised four parts: the headgroups, the alkyl chain spacers, the rigid mesogenic group, and the ester linker between the alkyl chains and the mesogenic group. In the present paper, in order to help understand the relationship between the molecular structure and the morphology obtained upon self-organization, a series of bolaamphiphiles has been designed and synthesized where each part has been systematically changed (see Figure 1).

Experimental Section

Materials. Muscovite mica purchased from United Mineral and Chemical in New York was freshly cleaved and used as the main substrate. Mica surfaces are negatively charged (1 per 0.48 nm^2) in water because of the dissociation of potassium counterions from mica lattice sites.[60,61] 6-Bromohexanoic acid, 8-bromooctanoic acid,

(41) Liang, K.; Hui, Y. *J. Am. Chem. Soc.* **1992**, *114*, 6588−6590.
(42) Wang, X.; Shen, Y.; Pan, Y.; Liang, Y. *Langmuir* **2001**, *17*, 3162−3167.
(43) Yan, Y.; Huang, J.; Li, Z.; Ma, J.; Fu, H.; Ye, J. *J. Phys. Chem. B* **2003**, *107*, 1479−1482.
(44) Yan, Y.; Xiong, W.; Huang, J.; Li, Z.; Li, X.; Li, N.; Fu, H. *J. Phys. Chem. B* **2005**, *109*, 357−364.
(45) Matsui, H.; Gologan, B. *J. Phys. Chem. B* **2000**, *104*, 3383−3386.
(46) Masuda, M.; Vill, V.; Shimizu, T. *J. Am. Chem. Soc.* **2000**, *122*, 12327−12333.
(47) Shimizu, T.; Masuda, M. *J. Am. Chem. Soc.* **1997**, *119*, 2812−2818.
(48) Duivenvoorde, F. L.; Feiters, M. C.; van der Gaast, S. J.; Engberts, J. B. F. N. *Langmuir* **1997**, *13*, 3737−3743.
(49) Visscher, I.; Engberts, J. B. F. N. *Langmuir* **2000**, *16*, 52−58.
(50) Gao, S.; Zou, B.; Chi, L. F.; Fuchs, H.; Sun, J. Q.; Zhang, X.; Shen, J. C. *Chem. Commun.* **2000**, 1273−1274.
(51) Zou, B.; Wang, L. Y.; Wu, T.; Zhao, X. Y.; Wu, L. X.; Zhang, X.; Gao, S.; Gleiche, M.; Chi, L. F.; Fuchs, H. *Langmuir* **2001**, *17*, 3682−3688.
(52) Zou, B.; Qiu, D. L.; Hou, X. L.; Wu, L. X.; Zhang, X.; Chi, L. F.; Fuchs, H. *Langmuir* **2002**, *18*, 8006−8009.
(53) Zou, B.; Wang, M. F.; Qiu, D. L.; Zhang, X.; Chi, L. F.; Fuchs, H. *Chem. Commun.* **2002**, 1008−1009.
(54) Qiu, D. L.; Song, B.; Lin, A. L.; Wang, C. Y.; Zhang, X. *Langmuir* **2003**, *19*, 8122−8124.
(55) Wang, M. F.; Qiu, D. L.; Zou, B.; Wu, T.; Zhang, X. *Chem. Eur. J.* **2003**, *9*, 1876−1880.
(56) Qiu, D. L.; Song, B.; Lin, A. L.; Wang, M. F.; Wang, Z. Q.; Zhang, X. *Chem. J. Chin. Univ.* **2004**, *25*, 2387−2389.
(57) Song, B.; Wang, Z. Q.; Chen, S. L.; Zhang, X.; Fu, Y.; Smet, M.; Dehaen, W. *Angew. Chem., Int. Ed.* **2005**, *44*, 4731−4735.
(58) Song, B.; Wei, H.; Wang, Z. Q.; Zhang, X.; Smet, M.; Dehaen, W. *Adv. Mater.* **2007**, *19*, 416−420.
(59) Israelachvili, J.; Wennerstrom, H. *Nature* **1996**, *379*, 219−225.
(60) Israelachivili, J. *Intermolecular & Surface Forces*, 2nd ed.; Harcourt Brace & Company Publishers: New York, 1992.
(61) Myers, D. *Surfaces, Interfaces, and Colloids: Principles and Applications*, 2nd ed.; John Wiley & Sons: New York, 1999.

10-bromodecanoic acid, 11-bromoundecanoic acid, 12-bromotridecanoic acid, 16-bromohexadecanoic acid, and 4,4′-hydroxybiphenyl were purchased from Aldrich. THF and toluene were distilled from sodium benzophenone ketyl, and triethylamine was distilled from potassium hydroxide prior to use.

As reported previously, BP-10 (refer to Figure 1) can form winding cylindrical surface micelles at the solution/mica interface, and these structures are stable during the drying process.[53,55] To identify the relationship between the molecular structure and self-organized interfacial morphology, herein, BP-10 was chosen as a reference molecule, and the bolaamphiphiles with different alkyl chain lengths, headgroups, rigid segments, as well as ester linkers were synthesized, as shown in Figure 1. The bolaamphiphiles with different lengths of alkyl chains were noted as BP-*n* (n = 5, 7, 9, 10, 11, and 15), where *n* stands for the number of methylene units. For the headgroups, bispyridinium was changed to bis-trimethylammonium (BP-10-TMA for short). For the rigid mesogenic groups, the biphenyl group was substituted with azobenzene (azo-10 and azo-11) or stilbene (stilbene-10). For the ester linkers, compounds BP-*r*-11 and azo-*r*-11 have been produced by directly binding the carbonyl group to the phenyl group, which was not the case for the other compounds (see Figure 1).

The bolaamphiphiles BP-5, BP-7, BP-9, BP-11, BP-15, BP-10-TMA, stilbene-10, azo-10, azo-11, and BP-*r*-11 were synthesized in a manner similar to work previously described according to the literature.[55] For reference, azobenzene-4,4′-dicarboxylic acid bis(pyridiniohexyl ester) dibromide (azo-*r*-11) was used, which was kindly provided by Prof. H. Ringsdorf.[6] 4,4′-Dihydroxyazobenzene was synthesized according to the literature.[62]

4,4′-Dihydroxybiphenylbis(6-pyridinium-*N*-yl-hexanoic ester) Dibromide (BP-5). ^{1}H NMR (300 MHz, DMSO, 25 °C, TMS): δ (ppm) = 9.13 (4H, d, J = 6.0 Hz, Ar−H ortho to N$^+$), 8.62 (2H, t, J = 7.8 Hz, Ar−H para to N$^+$), 8.18 (4H, d, Ar−H meta to N$^+$), 7.71 (4H, d, J = 8.6 Hz, Ar−H meta to C−OCO), 7.20 (4H, d, J = 8.6 Hz, Ar−H ortho to C−OCO), 4.65 (4H, t, J = 7.4 Hz, CH_2Py), 2.61 (4H, t, J = 7.3 Hz, CH_2COO), 2.00 (4H, m, CH$_2$CH_2-Py), 1.71 (4H, m, CH_2CH$_2$COO), 1.38 (4H, m, CH_2(CH$_2$)$_2$COO).

4,4′-Dihydroxybiphenylbis(8-pyridinium-*N*-yl-octanoic ester) Dibromide (BP-7). ^{1}H NMR (300 MHz, DMSO, 25 °C, TMS): δ (ppm) = 9.11 (4H, d, J = 5.5 Hz, Ar−H ortho to N$^+$), 8.62 (2H, t, J = 7.7 Hz, Ar−H para to N$^+$), 8.17 (4H, d, Ar−H meta to N$^+$), 7.70 (4H, d, J = 8.6 Hz, Ar−H meta to C−OCO), 7.21 (4H, d, Ar−H ortho to C−OCO), 4.63 (4H, t, J = 7.4 Hz, CH_2 Py), 2.60 (4H, t, J = 7.3 Hz, CH_2COO), 1.95−1.36 (20H, m, CH$_2$(CH_2)$_5$-CH$_2$COO).

4,4′-Dihydroxybiphenylbis(10-pyridinium-*N*-yl-decanoic ester) Dibromide (BP-9). ^{1}H NMR (300 MHz, DMSO, 25 °C, TMS): δ (ppm) = 9.08 (4H, d, J = 6.0 Hz, Ar−H ortho to N$^+$), 8.60 (2H, t, J = 7.8 Hz, Ar−H para to N$^+$), 8.15 (4H, d, J = 6.9 Hz, Ar−H meta to N$^+$), 7.70 (4H, d, J = 8.7 Hz, Ar−H meta to C−OCO), 7.20 (4H, d, J = 8.7 Hz, Ar−H ortho to C−OCO), 4.60 (4H, t, J = 7.5 Hz, CH_2Py), 2.60 (4H, t, J = 7.5 Hz, CH_2COO), 1.93−1.31 (28H, m, CH$_2$(CH_2)$_7$CH$_2$COO).

4,4′-Dihydroxybiphenylbis(11-pyridinium-*N*-yl-decanoic ester) Dibromide (BP-10). ^{1}H NMR (300 MHz, DMSO, 25 °C, TMS): δ (ppm) = 9.09 (4H, d, J = 6.0 Hz, Ar−H ortho to N$^+$), 8.60 (2H, t, J = 7.8 Hz, Ar−H para to N$^+$), 8.16 (4H, d, J = 6.9 Hz, Ar−H meta to N$^+$), 7.70 (4H, d, J = 8.7 Hz, Ar−H meta to C−OCO), 7.20 (4H, d, J = 8.7 Hz, Ar−H ortho to C−OCO), 4.60 (4H, t, J = 7.5 Hz, CH_2Py), 2.60 (4H, t, J = 7.5 Hz, CH_2COO), 1.92−1.29 (32H, m, CH$_2$(CH_2)$_8$CH$_2$COO).

4,4′-Dihydroxybiphenylbis(12-pyridinium-*N*-yl-tridecanoic ester) Dibromide (BP-11). ^{1}H NMR (300 MHz, DMSO, 25 °C, TMS): δ (ppm) = 9.10 (4H, d, J = 6.0 Hz, Ar−H ortho to N$^+$), 8.61 (2H, t, J = 7.8 Hz, Ar−H para to N$^+$), 8.16 (4H, d, J = 6.8 Hz, Ar−H meta to N$^+$), 7.70 (4H, d, J = 8.6 Hz, Ar−H meta to C−OCO), 7.21 (4H, d, J = 8.6 Hz, Ar−H ortho to C−OCO), 4.60 (4H, t, J = 7.4 Hz, CH_2Py), 2.60 (4H, t, J = 7.3 Hz, CH_2COO), 1.92−1.27 (36H, m, CH$_2$(CH_2)$_9$CH$_2$COO).

4,4′-Dihydroxybiphenylbis(16-pyridinium-*N*-yl-hexadecanoic ester) Dibromide (BP-15). ^{1}H NMR (300 MHz, DMSO, 25 °C, TMS): δ (ppm) = 9.07 (4H, d, J = 6.0 Hz, Ar−H ortho to N$^+$), 8.60 (2H, t, J = 7.8 Hz, Ar−H para to N$^+$), 8.15 (4H, d, J = 6.9 Hz, Ar−H meta to N$^+$), 7.70 (4H, d, J = 8.7 Hz, Ar−H meta to C−OCO), 7.20 (4H, d, J = 8.7 Hz, Ar−H ortho to C−OCO), 4.58 (4H, t, J = 7.5 Hz, CH_2Py), 2.59 (4H, t, J = 7.5 Hz, CH_2COO), 1.90−1.24 (52H, m, CH$_2$(CH_2)$_{13}$CH$_2$COO).

4,4′-Dihydroxybiphenylbis(11-trimethylammonium-*N*-yl-undecanoic ester) Dibromide (BP-10-TMA). The synthesis is similar with BP-ns, except that pyridine was replaced by trimethylamine. ^{1}H NMR (300 MHz, DMSO, 25 °C, TMS) = δ (ppm): 7.70 (4H, d, J = 8.7 Hz, Ar−H meta to C−OCO), 7.21 (4H, d, J = 8.7 Hz, Ar−H ortho to C−OCO), 3.26 (4H, t, J = 8.4 Hz, CH_2 N(CH_3)$_3$), 3.03 (18H, s, N(CH_3)$_3$), 2.60 (4H, t, J = 7.2 Hz, CH_2COO), 1.66−1.31 (32H, m, CH$_2$(CH_2)$_8$CH$_2$COO).

4,4′-Dihydroxystilbenebis(11-pyridinium-*N*-yl-undecanoic ester) Dibromide (Stilbene-10). ^{1}H NMR (300 MHz, DMSO, 25 °C, TMS): δ (ppm) = 9.08 (4H, d, J = 6.9 Hz, Ar−H ortho to N$^+$), 8.60 (2H, t, J = 7.8 Hz, Ar−H para to N$^+$), 8.15 (4H, d, J = 6.9 Hz, Ar−H meta to N$^+$), 7.64 (4H, d, J = 8.7 Hz, Ar−H ortho to CH═CH), 7.24 (2H, s, C*H*═C*H*), 7.12 (4H, d, J = 8.7 Hz, Ar−H meta to CH═CH), 4.59 (4H, t, J = 7.5 Hz, CH_2Py), 2.58 (4H, t, J = 7.5 Hz, CH_2COO), 1.92−1.28 (32H, m, CH$_2$(CH_2)$_8$CH$_2$COO).

4,4′-Dihydroxyazobenzenebis(11-pyridinium-*N*-yl-undecanoic ester) Dibromide (azo-10). ^{1}H NMR (300 MHz, DMSO, 25 °C, TMS): δ (ppm) = 9.09 (4H, d, J = 6.0 Hz, Ar−H ortho to N$^+$), 8.61 (2H, t, J = 7.8 Hz, Ar−H para to N$^+$), 8.16 (4H, d, J = 6.9 Hz, Ar−H meta to N$^+$), 7.96 (4H, d, J = 8.7 Hz, Ar−H ortho to N═N), 7.36 (4H, d, J = 8.7 Hz, Ar−H meta to N═N), 4.60 (4H, t, J = 7.5 Hz, CH_2Py), 2.63 (4H, t, J = 7.5 Hz, CH_2COO), 1.92−1.29 (32H, m, CH$_2$(CH_2)$_8$CH$_2$COO).

4,4′-Dihydroxyazobenzenebis(12-pyridinium-*N*-yl-dodecanoic ester) Dibromide (azo-11). ^{1}H NMR (300 MHz, DMSO, 25 °C, TMS): δ (ppm) = 9.09 (4H, d, J = 6.0 Hz, Ar−H ortho to N$^+$), 8.61 (2H, t, J = 7.8 Hz, Ar−H para to N$^+$), 8.16 (4H, d, J = 6.9 Hz, Ar−H meta to N$^+$), 7.96 (4H, d, J = 8.7 Hz, Ar−H ortho to N═N), 7.36 (4H, d, J = 8.7 Hz, Ar−H meta to N═N), 4.60 (4H, t, J = 7.5 Hz, CH_2Py), 2.63 (4H, t, J = 7.5 Hz, CH_2COO), 1.92−1.29 (36H, m, CH$_2$(CH_2)$_8$CH$_2$COO).

Biphenyl-4,4′-dicarboxylic acid bis(pyridinioundecyl ester) Dibromide (BP-*r*-11). ^{1}H NMR (300 MHz, DMSO, 25 °C, TMS): δ (ppm) = 9.10 (4H, d, J = 6.0 Hz, Ar−H ortho to N$^+$), 8.60 (2H, t, J = 7.8 Hz, Ar−H para to N$^+$), 8.16 (4H, d, J = 6.9 Hz, Ar−H meta to N$^+$), 8.06 (4H, d, J = 8.7 Hz, Ar−H ortho to C−COO), 7.90 (4H, d, J = 8.7 Hz, Ar−H meta to C−COO), 4.59 (4H, t, J = 7.5 Hz, CH_2Py), 4.39 (4H, t, J = 6.6 Hz, CH_2OCO), 1.92−1.29 (36H, m, CH$_2$(CH_2)$_9$CH$_2$OCO).

Synthesis of 4,4′-Dihydroxystilbene. Under nitrogen 2.2 g (10 mmol) of 4-iodophenol, 22 mg of Pd(OAc)$_2$ (0.1 mmol), 52 mg (0.2 mmol) of PPh$_3$, and 1.78 g (11 mmol) of 4-acetoxystyrene were dissolved in 50 mL of dioxane. The resultant mixture was refluxed for 24 h. After cooling to room temperature, the precipitate was filtered and the filtrate concentrated. The resulting residue was dissolved in 80 mL of THF/CH$_3$OH (1:1), and 4 g of NaOH in 20 mL of H$_2$O was added. Then the mixture was stirred for 12 h at room temperature. After adjusting the pH to 3 with HCl (1 mol/L), the solvent was removed and the crude product purified by a SiO$_2$ column using an ethyl acetate/CH$_2$Cl$_2$ mixture (1:1 v/v) as the eluent to give a pale yellow solid in 80% yield. ^{1}H NMR (300 MHz, DMSO, 25 °C, TMS): δ (ppm) = 7.35 (4H, d, J = 8.6 Hz, Ar−H ortho to CH═CH), 6.89 (2H, s, C*H*═C*H*), 6.74 (4H, d, J = 8.6 Hz, Ar−H meta to CH═CH).

Methods and Techniques. The critical micelle concentrations (CMC) were obtained from the plot of the conductivity as a function of the concentration. The conductivities were measured by DDS-307 conductivity meter produced by Shanghai Precision & Scientific Instrument Co. Ltd. Fourier transform infrared spectroscopy (FTIR) was performed with a Bruker IFS 66v/s spectrophotometer with an

(62) Wei, W.; Tomohiro, T.; Kodaka, M.; Okuno, H. *J. Org. Chem.* **2000**, *65*, 8979−8987.

Table 1. CMCs of the Diversified Bolaamphiphiles Involved[a]

1		2		3		4	
BP-5	×	BP-10	12.0	BP-10	12.0	BP-11	4.9
BP-7	40.0	azo-10	6.4	BP-10-TMA	6.5	BP-*r*-11	×
BP-9	22.0	stilbene-10	1.6			azo-11	4.0
BP-10	12.0					azo-*r*-11	0.34
BP-11	4.9						
BP-15	2.0						

[a] The right side of each column shows the corresponding CMCs. (×) No definite CMC measured.

attenuated total reflection (ATR) mode and recorded at a resolution of 2 cm^{-1} in vacuum with 512 scans. In measuring the IR spectra, all samples were made by dropping the solution on the mica substrate and drying in air before measurement. All ATR IR spectra were not smoothed. NMR spectra were recorded with a JOEL JNM-ECA300 apparatus.

The adsorbed interfacial micellar structures were observed by a commercial multimode Nanoscope IV atomic force microscope (AFM) produced by Veeco Instrument U.S. Company. Siliconnitride cantilevers MLCT-AUHW (Veeco Co., U.S.) with nominal spring constants of 0.06 N/m were used for tapping mode in fluid (f = 20−35 kHz) and silicon cantilevers RTESP (Veeco Co., U.S.) for tapping mode in air (f = 200−300 kHz). For in-situ measurements, the freshly cleaved mica sheet was mounted under the liquid cell, and the solutions were injected in the liquid cell and allowed to equilibrate for at least 10 min before the imaging. In-situ AFM images of surfactant aggregates were obtained with tapping mode in fluid. For ex-situ measurements, the freshly cleaved mica sheet was incubated in the aqueous solution for 10 min and then taken out and dried in air. Ex-situ AFM images of surfactant aggregates were acquired with tapping mode in air.

Results and Discussion

The values of CMC of the bolaamphiphile molecules measured by concentration-dependent conductivity are listed in Table 1. As shown in column 1 (Table 1), the CMC of the bolaamphiphiles decreases with the increase of the alkyl chain spacer length. This can be rationalized by the fact that hydrophobic interactions are enhanced with increasing number of methylene units. Therefore, the longer the spacer length, the smaller the amount of bolaamphiphile necessary to form micelles. For BP-5 that has only five methylene units, the slope of the concentration-dependent conductivity plot gradually increases with the concentration, but there is no obvious abrupt change, illustrating the absence of a definite CMC. This result suggests that the hydrophobic interactions between BP-5 molecules are so weak that micelles cannot form. BP-5 bolaamphiphiles should thus be considered as soluble. Besides the flexible alkyl chain, the rigid mesogenic groups also have a contribution to the hydrophobic interactions, and the aggregation of the mesogens is believed to be the reason for stabilizing the surface micellar structures.[51,53,55] When the biphenyl mesogen is replaced by azobenzene or stilbene, the CMC decreases, which may suggest that the interaction between these mesogens is different. As shown in column 3, the CMC of BP-10-TMA is lower than that of BP-10, which may be explained as the pyridinium is more easily to ionize than the TMA. Column 4 in Table 1 shows the CMCs of bolaamphiphiles that the orientation of the ester linkers is different from the bolaamphiphiles shown in Figure 1c. As will be shown below in the discussion of the effect of the rigid mesogenic group and the orientation of the ester linkers on the self-organization of the bolaamphiphiles, the orientation of the linkers can greatly influence the self-organization.

In the bulk solution, the self-organization of the amphiphiles is mainly driven by hydrophobic interactions between molecules. When the amphiphiles are adsorbed at the solid/liquid interfaces, hydrophobic interactions are not the only dominating driving force. Indeed, interactions between the molecules and solid interface are taking place. The cooperating effect of these two types of interactions acting on the amphiphiles may lead to a different self-organization behavior of the amphiphiles at the solid/liquid interface. Since all bolaamphiphiles studied are cationic (see Figure 1), negatively charged mica was chosen as the solid substrate. In the following sections, the effect of the different parts of the bolaamphiphiles on their self-organization behavior will be presented in detail. In order to make a proper comparison of the structure of the self-organized bolaamphiphiles at the interface and allow adsorption in equilibrium conditions, only concentrations above the CMC have been selected, typically approximately twice the value of the CMC.

Effect of the Alkyl Chain Spacer on the Self-Organization of the Bolaamphiphiles. In order to investigate the spacer effect, the methylene units of the alkyl chain are increased as follows: 5, 7, 9, 10, 11, and 15. The interfacial self-organized structures are observed by in-situ and ex-situ AFM, as shown in Figure 2 (due to the similarity, only typical examples of in-situ and ex-situ AFM images of BP-9, BP-11, and BP-15 are shown here). It seems that BP-9 forms a two-dimensional film when being observed by in-situ AFM, as shown in Figure 2a. BP-5 and BP-7, with shorter alkyl chain spacers, form similar structures (data not shown) to that of BP-9. As indicated in Figure 2c and e, BP-11 and BP-15 both form winding cylindrical micellar structures similar to that of BP-10.[53,55] Although a CMC has been measured for all of these bolaamphiphiles except for BP-5 (Table 1); only a winding cylindrical micellar structure has been obtained when the methylene units are equal to or larger than 10. These results indicate that the length of the alkyl spacer of the bolaamphiphiles is vital to formation of the surface micellar structure. The alkyl chains are responsible for the hydrophobic interactions that drive the amphiphilic molecules to self-organize into micelles in aqueous solution. The hydrophobic interactions will increase with elongation of the alkyl chain. Thus, it is easy to understand why formation of the winding cylindrical micellar structures can only happen when the alkyl chain is long enough.

For comparison, the stability of the self-organized structure during the dewetting process has been studied by ex-situ AFM. To do so, the freshly cleaved mica sheets were incubated in each bolaamphiphile solution for about 10 min, taken out and air dried, and then scanned with AFM. It is found that the winding cylindrical micellar structures formed by self-organization of BP-11 can still be obtained in the dry state as indicated in Figure 2d, just like what happens in the BP-10 system. This result indicates that the self-organized structure is stable during the drying process. For BP-9, which has shorter spacers, as shown in the AFM image in Figure 2b, there are adlayers with the layer thickness of about 3.7 nm, which is almost equal to the length of single molecules. Similar results also occur for BP-5 and BP-7 (data not shown). The adlayer structure should be formed by accumulation of the molecules in the dewetting process. For BP-15, which has relatively longer spacers, the winding cylindrical micellar structure present when hydrated could not be observed after drying even though different concentrations have been studied. Typical ex-situ AFM images are shown in Figure 2f. This result indicates that the bolaamphiphiles with too long spacers cannot retain their self-organized structures in the dewetting process. One rational explanation could be that elongation of the alkyl chain increases the flexibility of the chain, and the self-organized structure cannot maintain the aggregate morphology during the drying process. On the basis of the above results and

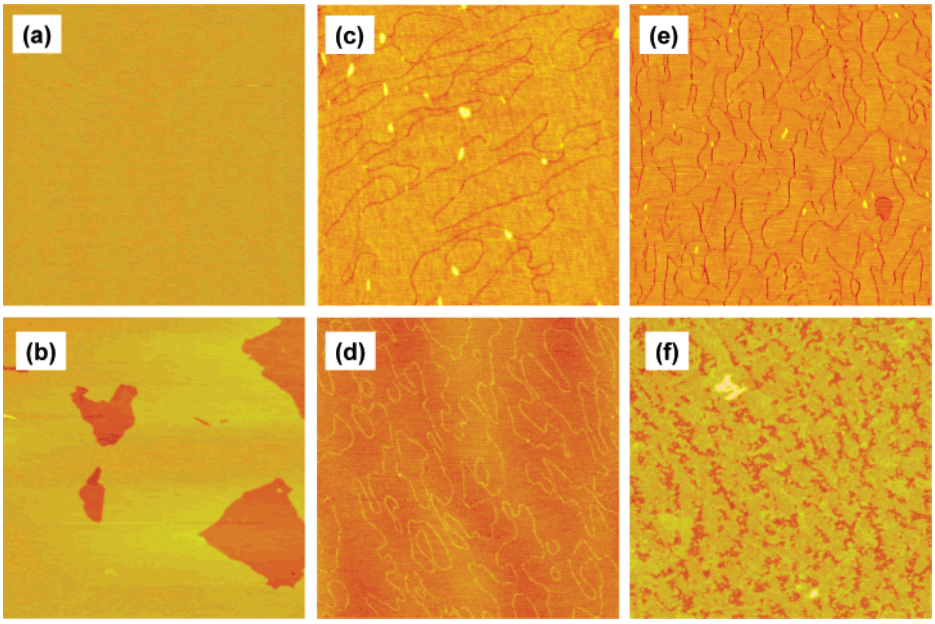

Figure 2. In-situ (top) and ex-situ (bottom) AFM images of BP-9 (a, b), BP-11 (c, d), and BP-15 (e, f). The scan area is 3 μm × 3 μm.

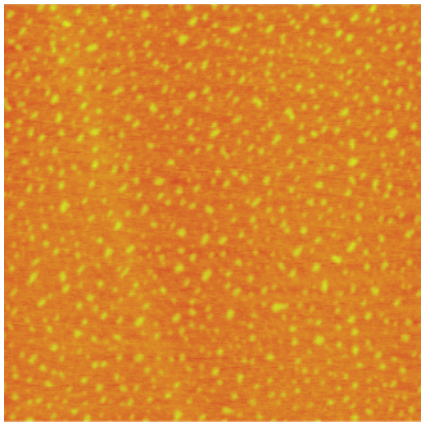

Figure 3. In-situ AFM observation of BP-10-TMA (scale of 3 μm × 3 μm).

analysis, we conclude that an appropriate length is necessary for formation of the stable surface micellar structures.

Effect of the Hydrophilic Headgroup on the Self-Organization of the Bolaamphiphiles. For the series of BP-*n* bolaamphiphiles, the headgroup is pyridinium. To investigate whether the pyridinium headgroup can influence the morphology of the self-organized surface structure, it is changed to TMA, and the resulting bolaamphiphile is called BP-10-TMA (Figure 1). As shown in Figure 3, BP-10-TMA forms dot-like structures at the mica/solution interface but multilayered structures are formed when this sample is dried (data not shown). The different self-organized structure observed for BP-10 and BP-10-TMA could be explained by the lower propensity of BP-10-TMA to aggregate because of the lack of π-conjugated aromatic pyridinium groups.

Effect of the Rigid Mesogenic Group and Orientation of the Ester Linkers on the Self-Organization of the Bolaamphiphiles. Previously, we demonstrated that azo-*r*-11[51,53] whose molecular structure is similar to BP-11 except that the mesogenic group is azobenzene and the orientation of the ester linker is different with BP-11 can form stripe-like structures when adsorbed at the mica/solution interface. Though these two molecules are both bolaamphiphiles bearing mesogenic groups, their self-organized surface structures are distinctly different, as shown in Figure 2c for BP-11, Figure 5b for azo-*r*-11. In order to understand the mechanism behind such a distinct change, two groups of

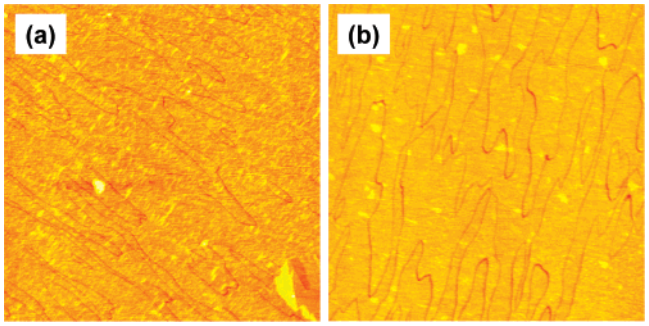

Figure 4. In-situ AFM observations of (a) stilbene-10 and (b) azo-10. The scan area is 3 μm × 3 μm.

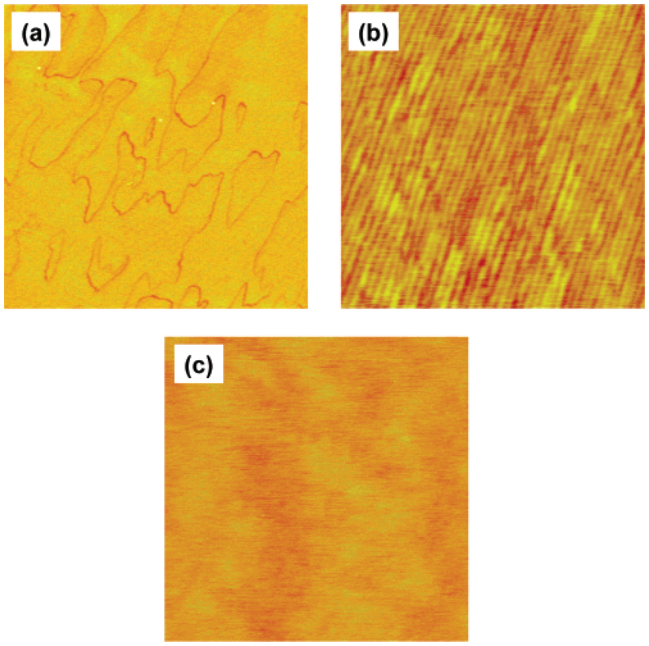

Figure 5. In-situ AFM observations of (a) azo-11 (3 μm × 3 μm), (b) azo-*r*-11 (600 nm × 600 nm), and (c) BP-*r*-11 (3 μm × 3 μm).

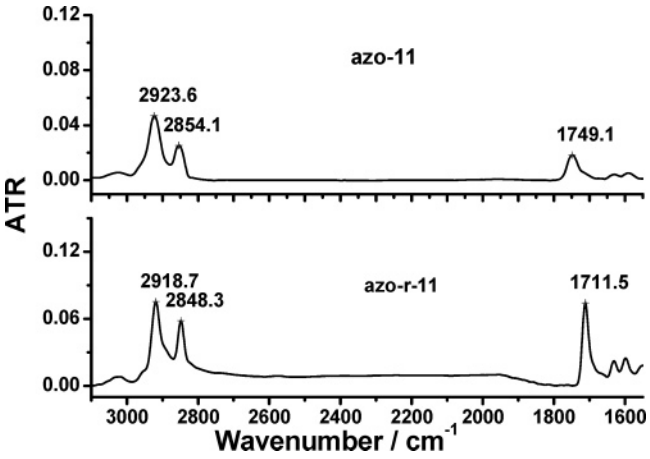

Figure 6. ATR FTIR spectra of azo-11 and azo-*r*-11.

experiments have been done by separately changing the mesogenic group and the orientation of the ester linkers.

When the biphenyl mesogen is replaced by azobenzene or stilbene, the bolaamphiphiles are noted as azo-10 and stilbene-10, respectively. As shown in Figure 4, azo-10 and stilbene-10 both form the winding cylindrical micellar structures at the mica/solution interface, which are similar to that formed by self-organization of BP-10. These results indicate that changing the biphenyl rigid mesogen group to either azobenzene or stilbene has little effect on the self-organized surface structure in this case. It is worth to noting that though these three bolaamphiphiles all can form the winding cylindrical micellar structures at the mica/solution interface, their CMCs are different, reflecting that biphenyl, azobenzene, and stilbene have different contributions to the hydrophobicity of the bolaamphiphiles.

Since the difference between the self-organized surface structures of the BP-11 and azo-r-11 is not mainly due to the type of mesogenic group, the effect of the orientation of the ester linker has been studied. Therefore, two pairs of molecules have been compared: azo-11 and azo-*r*-11 as well as BP-11 and BP-*r*-11, where *r* refers to the structure where the carbonyl group is directly connected to the phenyl group. For the bolaamphiphiles bearing azobenzene groups, azo-11, which bears an alkyl chain slightly larger than that of azo-10, also self-organizes into winding cylindrical micellar structures (Figures 5a) at the mica/solution interface, while azo-*r*-11 forms stripe-like structure (Figure 5b). This difference can also be explained by the CMC and FTIR spectra of these compounds. The CMC of azo-*r*-11 is much lower than that of azo-11, suggesting that azo-*r*-11 more easily self-organizes as aggregate. As for the ATR FTIR shown in Figure 6, the positions of the band at 2918.7 and 2848.3 cm^{-1}, respectively, assigned to the C−H asymmetric and symmetric stretching vibration of CH_2 indicate that the alkyl chains of azo-*r*-11 are highly ordered (trans conformation).[63−66] The asymmetric and symmetric stretching vibrations of CH_2 in azo-11 are at around 2923.6 and 2854.1 cm^{-1}, indicating that there are a larger number of gauche conformers in the alkyl chains. It should be pointed out that the bandwidths of azo-11 at 2923.6 and 2854.1 cm^{-1} are larger than that of the corresponding peaks of azo-*r*-11, which suggests an increased mobility of the alkyl chain in azo-11.[65,66] In addition, the C═O stretching band of azo-*r*-11 peaks around 1711.5 cm^{-1} due to the conjugation with the mesogenic group, whereas the C═O stretching band of azo-*r*-11 peaks around 1749.1 cm^{-1}. These data provide evidence that azo-*r*-11 can self-organize to form higher ordered structures than azo-11. For the bolaamphiphile BP-*r*-11 that contains a biphenyl group, we did not get winding cylindrical micellar structure at the mica/solution interface but obtained a two-dimensional film as shown in Figure 5c. Comparing with the azo system, BP-*r*-11 has a good solubility and does not show a definite CMC. These results indicate the orientation of the ester linker has a great effect on the interfacial self-organization behavior of the bolaamphiphiles.

Conclusions

We designed and synthesized a series of bolaamphiphiles bearing mesogenic groups and investigated the interfacial self-organization behavior of these molecules. Our experiments have shown that an appropriate alkyl chain length is necessary to form a closely packed structure. The type of headgroup as well as the orientation of the ester linker between the mesogenic group and the alkyl chain can greatly influence the interfacial self-organization of this kind of bolaamphiphiles. This work may be helpful for the molecular engineering of bolaamphiphiles to form tailor-made surface morphologies.

Acknowledgment. The authors thank the National Basic Research program of China (2007CB808000), the National Natural Science Foundation of China (20574040, 20334010, 20473045, 50703022), the Postdoctoral Science Foundation of China (20060390055), and the Ministry of Education for financial support.

LA7030158

(63) Miyahara, M.; Kawasaki, H.; Fukuda, T.; Ozaki, Y.; Maeda, H. *Colloids Surf., A: Physicochem. Eng. Aspects* **2001**, *183*, 475−485.
(64) Zhang, X.; Li, H. B.; Zhao, B.; Shen, J. C.; Gao, Z. M.; Li, X. S. *Macromolecules* **1997**, *30*, 1633−1636.
(65) Sapper, H.; Cameron, D. G.; Mantsch, H. H. *Can. J. Chem.* **1981**, *59*, 2543−2549.
(66) Umemura, J.; Cameron, D. G.; Mantsch, H. H. *Biochim. Biophys. Acta* **1980**, *602*, 32−44.